



Get Clarity On Generics

Cost-Effective CT & MRI Contrast Agents



FRESENIUS
KABI

WATCH VIDEO

AJNR

Characterization of intracranial mass lesions with in vivo proton MR spectroscopy.

H Poptani, R K Gupta, R Roy, R Pandey, V K Jain and D K Chhabra

AJNR Am J Neuroradiol 1995, 16 (8) 1593-1603

<http://www.ajnr.org/content/16/8/1593>

This information is current as
of August 15, 2025.

Characterization of Intracranial Mass Lesions with In Vivo Proton MR Spectroscopy

Harish Poptani, Rakesh K. Gupta, Raja Roy, Rakesh Pandey, Vijayendra K. Jain, and Devendra K. Chhabra

PURPOSE: To assess the use of in vivo proton MR spectroscopy for characterization of intracranial mass lesions and to ascertain its reliability in grading of gliomas. **METHODS:** One hundred twenty patients with intracranial masses were subjected to volume selective spectroscopy using stimulated echo acquisition mode (echo time, 20 and 270 milliseconds) and spin echo (echo time, 135 milliseconds) sequences. The intracranial lesions were grouped into intraaxial and extraaxial, as judged with MR imaging. Assignment of resonances was confirmed in two samples each of brain abscess, epidermoid cyst, and tuberculoma using ex vivo high-resolution MR spectroscopy. **RESULTS:** The in vivo spectra appeared distinct compared with normal brain in all the cases. All high-grade gliomas ($n = 37$) showed high choline and low or absent *N*-acetyl-L-aspartate and creatine along with lipid and/or lactate, whereas low-grade gliomas ($n = 23$) were characterized by low *N*-acetyl-aspartate and creatine and high choline and presence of only lactate. *N*-acetyl-aspartate/choline ratio was significantly lower and choline/creatine ratio was significantly higher in high-grade gliomas than in low-grade gliomas. Presence of lipids suggested a higher grade of malignancy. All metastases ($n = 7$) showed lipid and lactate, whereas choline was visible in only four cases. Epidermoids showed resonances from lactate and an unassigned resonance at 1.8 ppm. Meningiomas could be differentiated from schwannomas by the presence of alanine in the former. Among the infective masses, pyogenic abscesses ($n = 6$) showed resonances only from cytosolic amino acids, lactate, alanine, and acetate; and tuberculomas ($n = 11$) showed only lipid resonances. **CONCLUSIONS:** In vivo proton MR spectroscopy, helps in tissue characterization of intracranial mass lesions. Spectroscopy is a reliable technique for grading of gliomas when *N*-acetyl-aspartate/choline and choline/creatine ratios and presence of lipids are used in combination.

Index terms: Magnetic resonance, spectroscopy; Brain neoplasms, magnetic resonance

AJNR Am J Neuroradiol 16:1593–1603, September 1995

In vivo proton magnetic resonance (MR) spectroscopy, a noninvasive technique, has been helpful in understanding the pathophysiology of the different disease processes (1). It has been used to observe metabolite changes in different intracranial abnormalities such as tumors, stroke, tuberculomas, multiple sclerosis,

and metabolic brain disorders (1, 2). Spectroscopic studies on brain tumors have attempted to (a) characterize the different histologic types and (b) predict the degree of malignancy of the gliomas (3–11). Preoperative grading of gliomas is necessary, because it helps in better treatment planning and management. Imaging modalities such as computed tomography and MR are unreliable in the grading of different gliomas (12).

We present our experience with proton MR spectroscopy in 120 patients with histologically different types of mass lesions. The study was performed with the aims of studying the spectral difference between neoplastic versus infective mass lesions, and assessing its reliability in differentiating high-grade (grade III–IV) from low-grade (grade I–II) gliomas.

Received November 16, 1994; accepted after revision April 17, 1995.

From the Departments of Radiology (H.P., R.K.G.), Pathology (R.P.), and Neurosurgery (V.K.J., D.K.C.) Sanjay Gandhi Post Graduate Institute of Medical Sciences and the Regional Sophisticated Instrument Centre (R.R.), Central Drug Research Institute, Lucknow, India.

Address reprint requests to Rakesh K. Gupta, MD, Associate Professor, MR Section, Department of Radiology, Sanjay Gandhi PGIMS, Lucknow-226 014 India.

AJNR 16:1593–1603, Sep 1995 0195-6108/95/1608–1593

© American Society of Neuroradiology

Subjects and Methods

One hundred twenty patients with intracranial mass lesions, suggested by MR, were selected for proton MR spectroscopy; 85 were male and 35 female. The majority of them ranged in age from 12 to 65 years ($n = 110$); the remaining were between 2 and 12 years of age ($n = 9$) and younger than 2 years ($n = 1$). Informed consent was obtained from all the subjects/guardians before the study. A lesion size of more than 8 mL (on MR) was the inclusion criterion for selection of patients for proton MR spectroscopy. Using the MR criteria of Curnes (13), the lesions were classified as intraaxial or extraaxial. Histologic diagnosis of all the cases was obtained by stereotactic biopsy or craniotomy and open biopsy, except six cases of intracranial tuberculomas that presented with tuberculous meningitis. The diagnosis in these patients was based on MR features, cerebrospinal fluid findings, presence of extracranial tuberculosis stigmata, and response to specific treatment (14–16).

Gliomas of different histologic types were graded I to IV, according to the degree of malignancy. Grade I and II gliomas were taken together as low-grade, and grade III and IV were high-grade gliomas (5, 17). Among the 23 low-grade gliomas, 16 were totally solid, and 7 had variable cystic components. Of the 37 high-grade gliomas 29 were solid and the remaining 8 had small areas of cyst formation or necrosis.

All patients and age- and sex-matched healthy controls were subjected to MR and proton MR spectroscopy in one sitting. The study was performed on a whole body system at 1.5 T, using a circularly polarized head coil. In pediatric cases, sedation was given in appropriate doses.

MR Imaging

Multipolar T1- and T2-weighted images, using spin-echo sequence, were obtained in all the patients. Postcontrast study was performed in all cases except in epidermoid, dermoid, and arachnoid cysts and cranio-pharyngioma and chromophobe adenomas when the lesion appeared clearly discernible and thus the contrast study was not needed.

Proton MR Spectroscopy

In vivo study. A volume of interest of 4.09 to 8.0 mL was selected from the center of the lesion with edges of the voxel well within the mass. The volume of interest chosen was confirmed by taking turbo fast low-angle shot images with sequence parameters of 6.5/3/1 (repetition time/echo time/excitations), with inversion time of 500 and 80° flip angle, in the three orthogonal planes. To ensure that the subject had not moved during the study, the volume of interest was once again confirmed by imaging after the spectroscopic study was over.

Single voxel proton MR spectroscopy was performed using stimulated echo acquisition mode (STEAM) with three chemical shift selective pulses for water suppression

(18). The bandwidth of the chemical shift selective pulses was 60 Hz. STEAM sequence parameters used for the study were 3000/20/128 with 27.5 milliseconds mixing time, and 3000/270/128 with 27.5 milliseconds mixing time, with an acquisition time of 6.5 minutes each using a gradient strength of 3 mT/m. In 40 of 120 cases, a spin-echo sequence (19) with parameters of 3000/135/256 and an acquisition time of 13 minutes, also was performed. Sequences with different echo times were run to (a) identify resonances with short T2 values, (b) observe and confirm the phase reversal shown by J coupled metabolites, and (c) confirm the presence or absence of lipid/*N*-acetyl-L-aspartate (NAA) peak at 2.02 ppm, because at a longer echo time of 270 milliseconds, only the NAA peak would be visible. Voxel shimming of the free induction decay signal without water suppression yielded a line width (full width at half maximum) of 4 to 6 Hz. Total time taken for imaging and spectroscopy ranged between 80 and 90 minutes.

Postprocessing of the free induction decay included zero filling to 4K data points followed by Gaussian multiplication for resolution enhancement. The resulting free induction decay was Fourier transformed and phase corrected, and no baseline correction was done. The signal intensity ratios of NAA/choline (Cho), NAA/creatine (Cr), and Cho/Cr were calculated from the STEAM 20-millisecond spectrum.

Assignment of resonances seen *in vivo* was done according to literature reports of these peaks at 1.5 T (20) or from reports of *ex vivo* studies (21, 22). The resonance at 1.3 ppm was assigned to lactate if it showed a line width comparable to other metabolite peaks in the spectrum, a coupling constant of 7 Hz, and a phase reversal at the spin-echo 135-millisecond spectrum. On the other hand, if the peak at 1.3 ppm was broad, exhibited no phase reversal at the spin-echo 135-millisecond spectrum, and showed a marked reduction in the signal intensity at STEAM 270-millisecond spectrum, it was assigned to lipids (23). If a broad resonance was observed at 1.3 ppm on the STEAM 20-millisecond spectrum and showed a phase reversal at spin-echo 135 millisecond and a significant reduction in the signal intensity at STEAM 270-millisecond spectrum, it was attributed to lipids and lactate.

Comparison of the spectroscopic results from these intracranial mass lesions was done by studying the contralateral uninvolved part of the brain wherever possible. In addition, data from 40 healthy volunteers from different volumes of interest also were obtained for statistical evaluation.

Absolute quantification of metabolites taking water as an internal reference is sensitive to distortions of the strong water resonance in the reference acquisition without water suppression. This severely complicates the exact definition of the boundaries for signal integration. Quantification using an external standard, in the form of a physiologic phantom, is limited by its own drawbacks such as coil loading factor, capillary volume fraction, and cerebrospinal fluid volume fraction (24). Thus, in the present study

we have taken metabolite ratios as a compromise for absolute quantification.

Ex vivo study. In two cases, each of tuberculoma, abscess, and epidermoid cyst, ex vivo proton MR spectroscopy was carried out on a 400-MHz MR spectrometer to confirm the assignment of resonances seen in vivo. The excised tissue/pus was immediately frozen in liquid nitrogen. The thawed samples then were directly introduced in 5-mm MR tubes and 500 μ L D₂O (containing 0.75% 3-[Trimethylsilyl]propionic-2,2,3,3-d₄ acid, sodium salt, TSP) was added to these samples. The sequence parameters for pulse collect spectrum included a repetition time of 5000 milliseconds, pulse angle of 90°, spectral width of 4000 Hz, vector size of 16 k data points, and 128 excitations. To confirm the presence of J coupled metabolites, a Hahn spin-echo sequence with 5000/100/128 and 16 k data points also was performed.

Statistical evaluation. NAA/Cho, Cho/Cr, and NAA/Cr ratios in low- and high-grade gliomas were compared using Student's *t* test, because these ratios followed the normal distribution when test of normality was applied.

Results

The spectra from the contralateral brain or from the healthy volunteers revealed a consistent pattern of the four major peaks of NAA, Cr, Cho, and myoinositol (ml) (Fig 1B). No lactate or lipid resonances were visible in any of the healthy subjects studied. The mean NAA/Cho, NAA/Cr, and Cho/Cr ratios from the 40 volunteers were 1.85 ± 0.15 , 1.48 ± 0.32 , and 0.82 ± 0.09 , respectively.

Intraaxial Mass Lesions

All 23 low-grade gliomas showed increased Cho and reduced NAA resonances, with a mean NAA/Cho ratio of 0.39 ± 0.12 in 23 cases. Lactate was seen in all the low-grade gliomas, whereas lipid resonance was not seen in any of these tumors (Fig 1C).

Among the 37 high-grade gliomas, NAA and Cr peaks were visible in only 12 of 37 cases and were undetectable in the remaining 25 cases. The mean NAA/Cho ratio in the 12 cases was 0.19 ± 0.08 . The ratios were not calculated in the remaining 25 cases, because an assumed value of zero signal intensity of NAA and Cr would have lead to ambiguous results (eg, Cho/Cr = infinity for Cr = 0). Most of the high-grade gliomas showed the presence of lipids and lactate (n = 25), with only lactate in 10 and only lipids (Fig 2B) in two cases.

When compared, the difference in the NAA/Cho and Cho/Cr ratios between low- and high-grade gliomas were statistically significant (Table 1).

The presence of lipid and lactate resonance at 1.3 ppm was seen in all seven cases of metastasis. Cho resonance was seen in only four cases, and a small peak at 2.02 ppm was seen in five cases, which was attributed to lipids (Fig 3B).

Both cases of multicentric primary lymphomas showed high Cho and lipid/lactate resonances at 1.3 ppm with no NAA and Cr.

TABLE 1: Metabolite signal intensity ratios from STEAM 20-millisecond spectrum

Ratio	High Grade (n = 12)			Low Grade (n = 23)			P value
	Mean	SD	SEM	Mean	SD	SEM	
NAA/Cho	0.1927	0.0819	0.0246	0.3943	0.1241	0.0331	5.7×10^{-5}
Cho/Cr	2.9107	1.0801	0.2886	2.0650	0.7555	0.2181	1.6×10^{-2}
NAA/Cr	0.4175	0.2427	0.0858	0.7609	0.2968	0.0894	0.2051*

* Not significant.

Extraaxial Mass Lesions

The presence of alanine peaks at 1.5 ppm was seen in 12 of the 13 cases of meningioma. In addition, all the cases showed strong Cho resonance. In 6 cases, small resonance from lactate also was observed (Fig 4B).

Alanine and NAA were not visible in any of the eight cases of schwannoma studied. Lipids and/or lactate was seen in only three cases, whereas increased Cho was observed in all the cases.

Epidermoid cysts (n = 8) showed an overall reduced signal intensity compared with other tumors. A characteristic spectral pattern of lactate at 1.3 ppm along with a small peak at 1.8 ppm was seen in all the cases (Fig 5B). No other metabolite signal was observed at stimulated echo acquisition mode 20. The presence of the peak at 1.8 ppm was confirmed by the ex vivo spectra (Fig 5C), but no definite assignment could be done.

Both cases of arachnoid cyst did not show any other metabolite resonance except for a very small lactate peak.

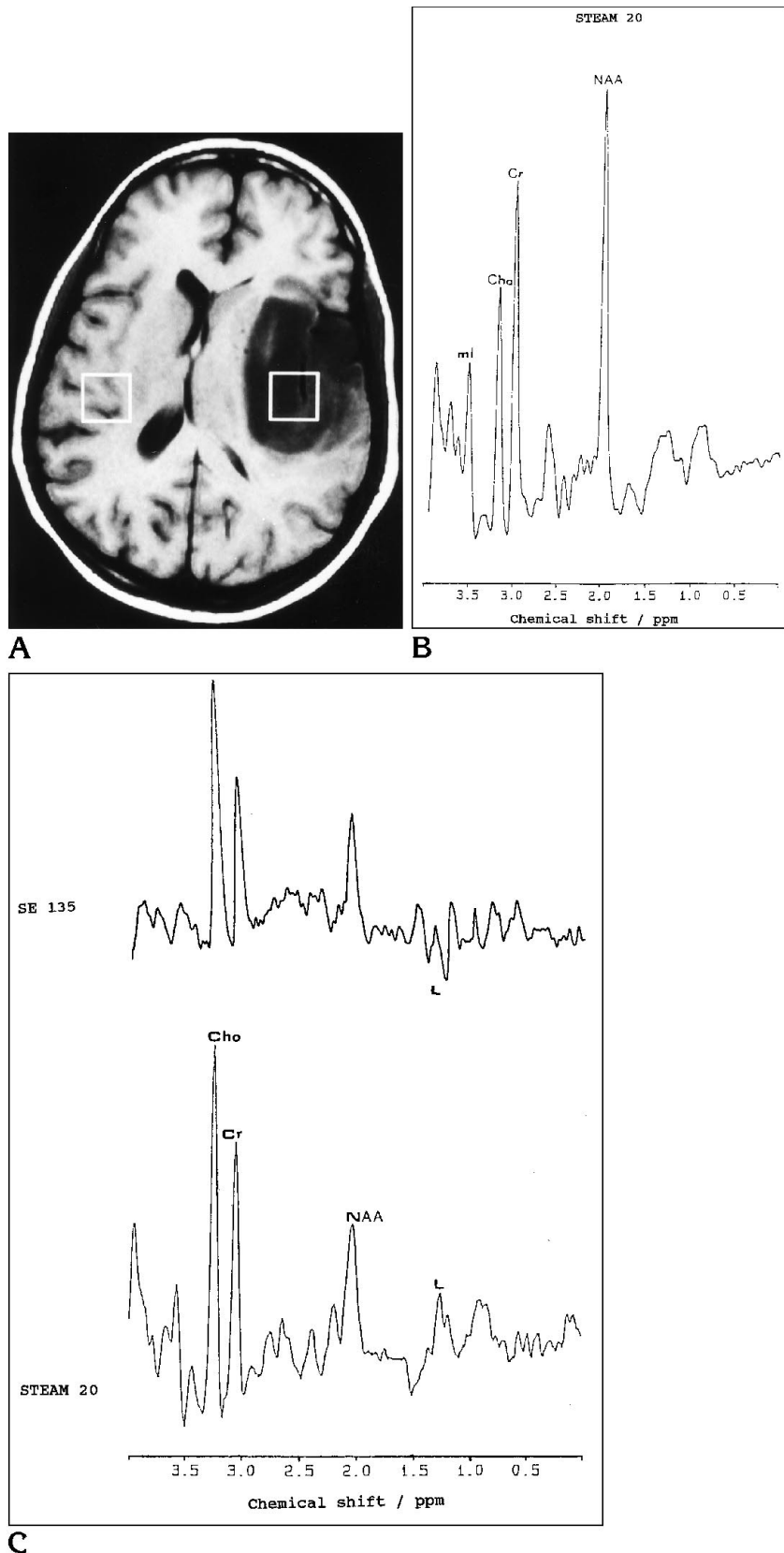
The single case of a dermoid cyst exhibited very strong and broad resonances from mobile lipids at 0.9 and 1.3 ppm. No other metabolite was seen.

A case of craniopharyngioma showed only

Fig 1. Astrocytoma grade II. A, T1-weighted axial image (600/15/2) shows predominantly hypointense lesion in the left parietal area with mass effect.

B, Spectrum of the normal contralateral (right) region at 20 milliseconds shows major resonances at 2.02, 3.02, 3.22, and 3.56 ppm.

C, Spectra from the center of the lesion (inset) shows decrease in the NAA and Cr with increased Cho peak and a doublet at 1.3 ppm assigned to lactate (L). Note the phase reversal of resonance at 1.3 ppm at spin-echo (SE) 135.



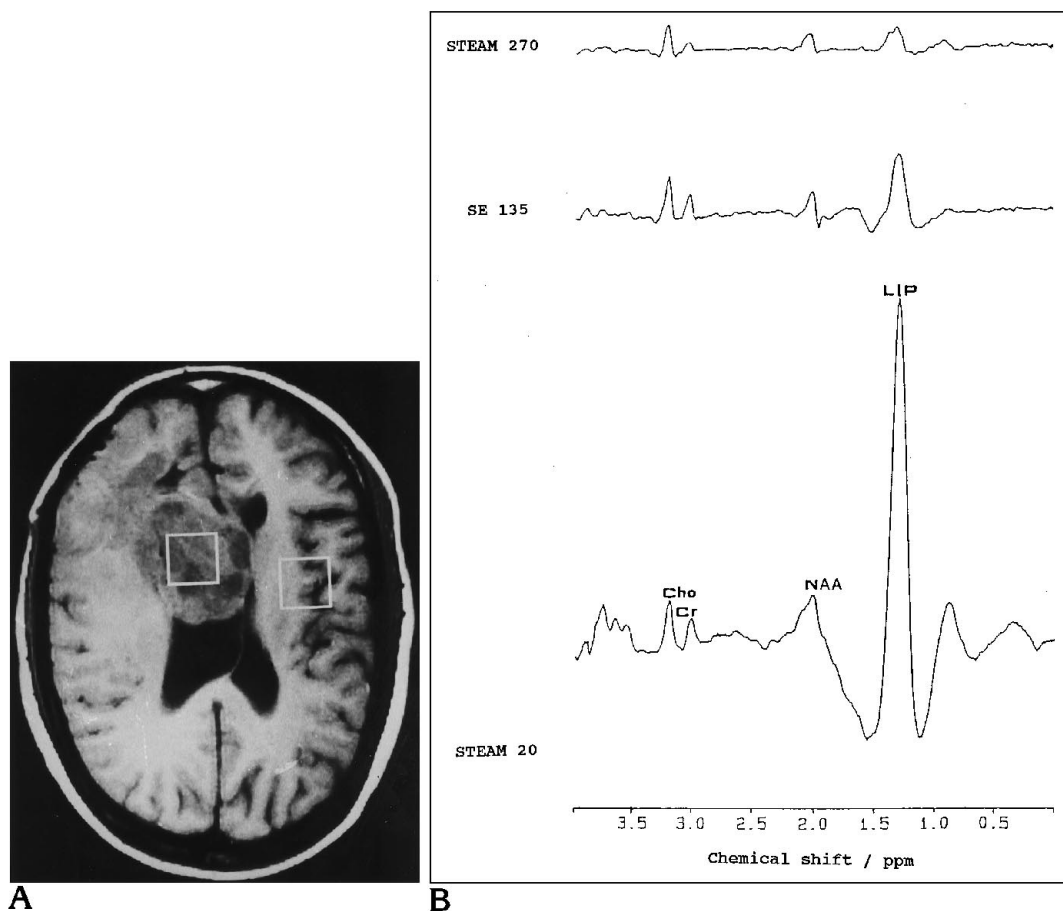


Fig 2. Glioblastoma multiforme. A, T1-weighted axial image (600/15/2) shows mixed-intensity mass involving the right frontal region extending into the ipsilateral ventricle with mass effect.

B, Spectra from the tumor (inset) shows broad and large resonances at 1.3 ppm, along with small resonances from NAA, Cr, and Cho. The resonance at 1.3 ppm shows marked reduction in the signal with no phase reversal at spin-echo (SE) 135 and a further reduction at STEAM 270. All three spectra are plotted on the same scale. LIP indicates lipid.

lactate, whereas chromophobe adenoma exhibited only noise, and no metabolite resonances were observed.

Nonneoplastic Lesions

All 6 pyogenic abscesses exhibited strong resonances at 0.9 ppm, 1.3 ppm (lactate), 1.5 ppm (alanine), and 1.92 ppm (acetate) with absence of NAA, Cho, and Cr peaks (Fig 6B). The broad resonance seen at 0.9 ppm in the in vivo spectrum was assigned to cytosolic amino acid residues (valine, leucine, not resolvable at 1.5 T) by high-resolution ex vivo MR study (Fig 6).

All 11 cases of tuberculoma showed presence of strong lipid resonances at 0.9 and 1.3 ppm. No other metabolite peaks were observed.

Metabolite changes in different neoplastic

and nonneoplastic intracranial mass lesions are summarized in Table 2.

Discussion

NAA is a neuronal marker and decreases in all tumors because of the invasiveness of tumor cells within the normal tissue (9). Proton MR spectroscopy-visible Cho-containing compounds include acetyl choline, glycerophosphocholine, and phosphocholine (1). Cho is increased in all tumors (4, 8) because of increased membrane turnover and cell proliferation. Cr/phosphocreatine, an indicator of energy metabolism, shows a variable signal intensity in proton MR spectroscopy of intracranial tumors (5, 9). Gliomas have been graded on the basis of NAA/Cho (9–11), Cho/Cr, NAA/Cr (6), and lactate/Cr (5) ratios. NAA/

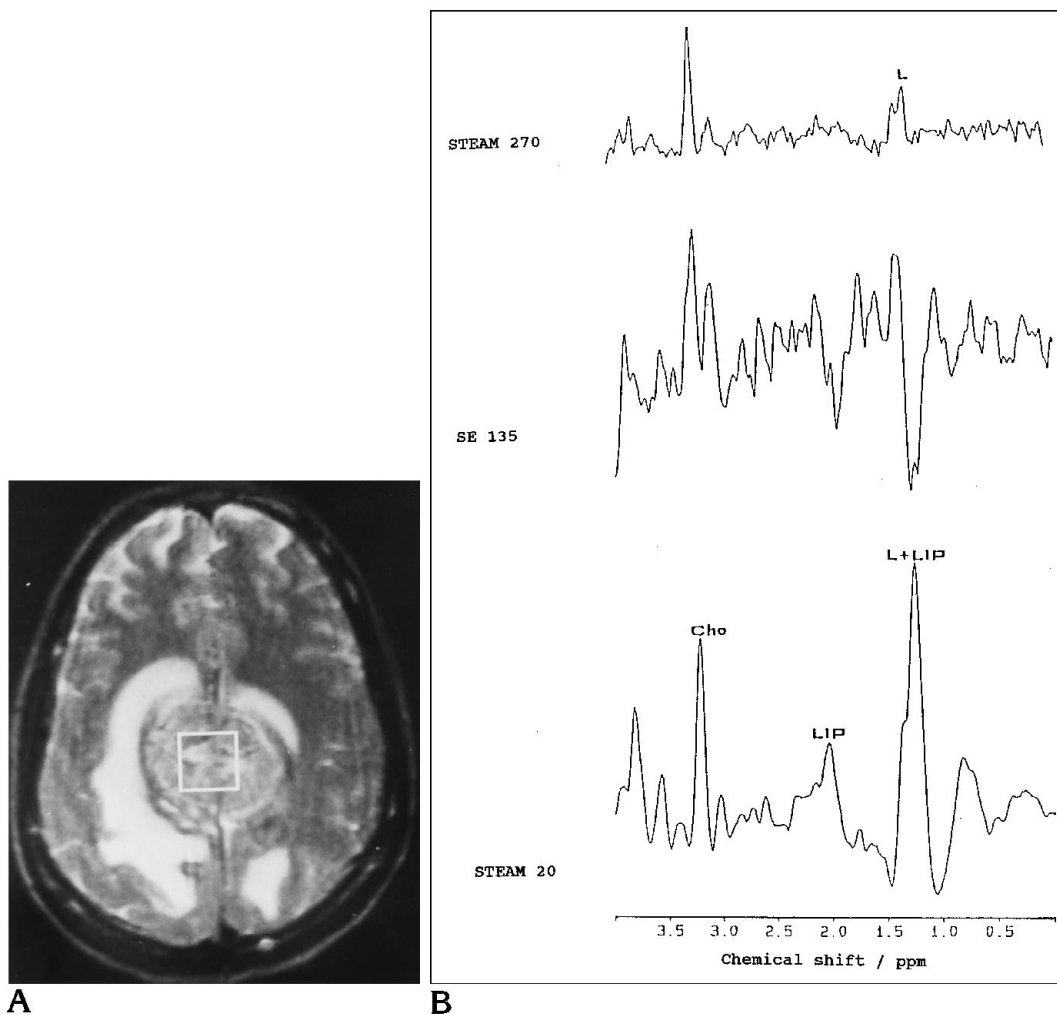


Fig 3. Metastatic adenocarcinoma (primary from breast). A, T2-weighted axial image (2200/80/1) shows a mixed-intensity mass lying in the center, extending on either side. It is associated with perifocal edema.

B, Spectra at echo time 20 shows broad resonance at 1.3 ppm and 2.02 ppm and Cho at 3.22 ppm. At spin-echo (SE) 135, the resonance at 1.3 ppm shows phase reversal, and at STEAM 270, the resonance at 2.02 disappears, confirming it to have a small T2 value and thus be from lipids (LIP). L indicates lactate.

Cho and Cho/Cr ratios have shown consistency in predicting the tumor grade (6, 10, 11). We observed NAA peak in only 12 of 37 cases of high-grade gliomas. The comparison of NAA/Cho and Cho/Cr ratios in these cases with that of the low-grade gliomas provided a significant difference between the two groups. In the present study, NAA/Cr ratio did not provide any significant correlation with the degree of malignancy. Most tumor cells have low respiration and high glycolysis rates even when oxygen levels are sufficient for respiration. The high glycolytic rate results in increased accumulation of pyruvate, which converts to lactate, because there is a decrease in the tricarboxylic acid cycle activity in brain tumors (25, 26).

Alternatively, lactate also may be produced by anaerobic glycolysis in tumors with hypoxia. Increased lactate is found in both the high- and low-grade gliomas (9). Lactate in all the low-grade gliomas and most high-grade gliomas in the present study suggests that its presence does not correlate with the grade of malignancy.

Lipid resonances have been observed in high-grade gliomas on in vivo studies using different echo times, especially in areas of MR imaging-detectable necrosis (Lazeyras F, Charles HC, Boyko O, Frederiks R, Schold C, Coleman RE, "New Perspectives in Tumor Grading by Combined Short Echo/Long Echo ^1H Spectroscopic Imaging," presented at the 11th Annual Meeting of the Society of Magnetic

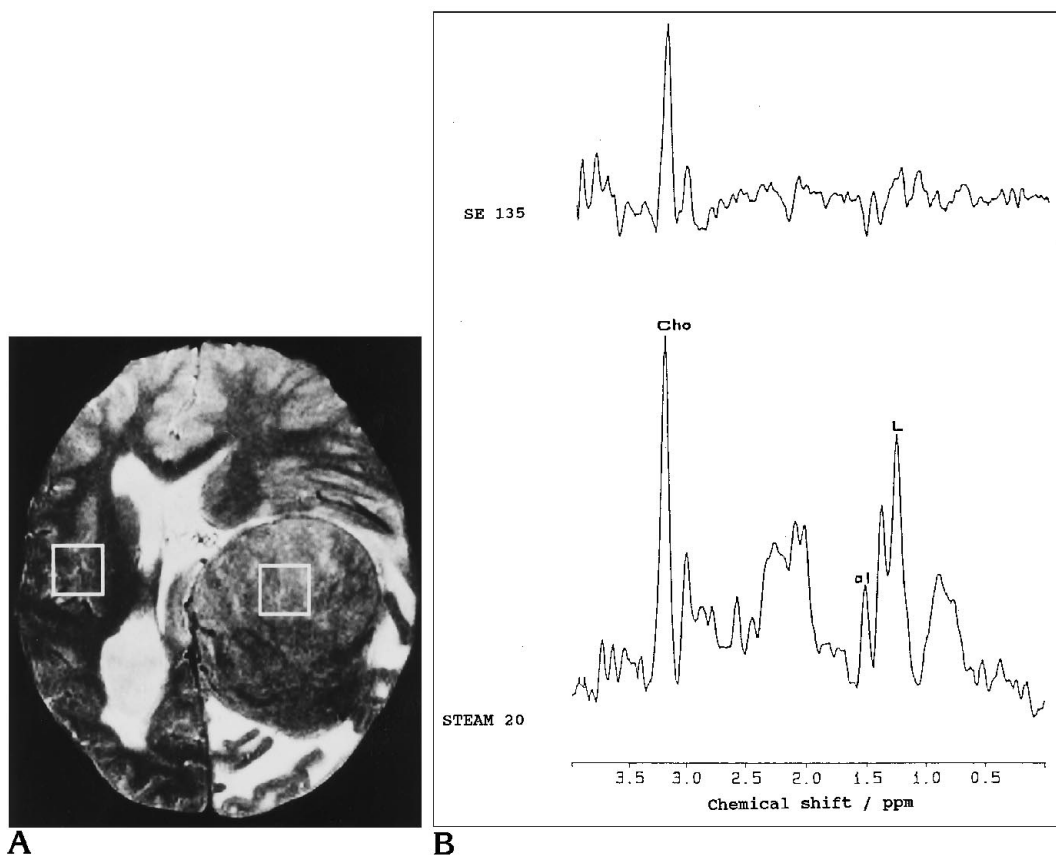


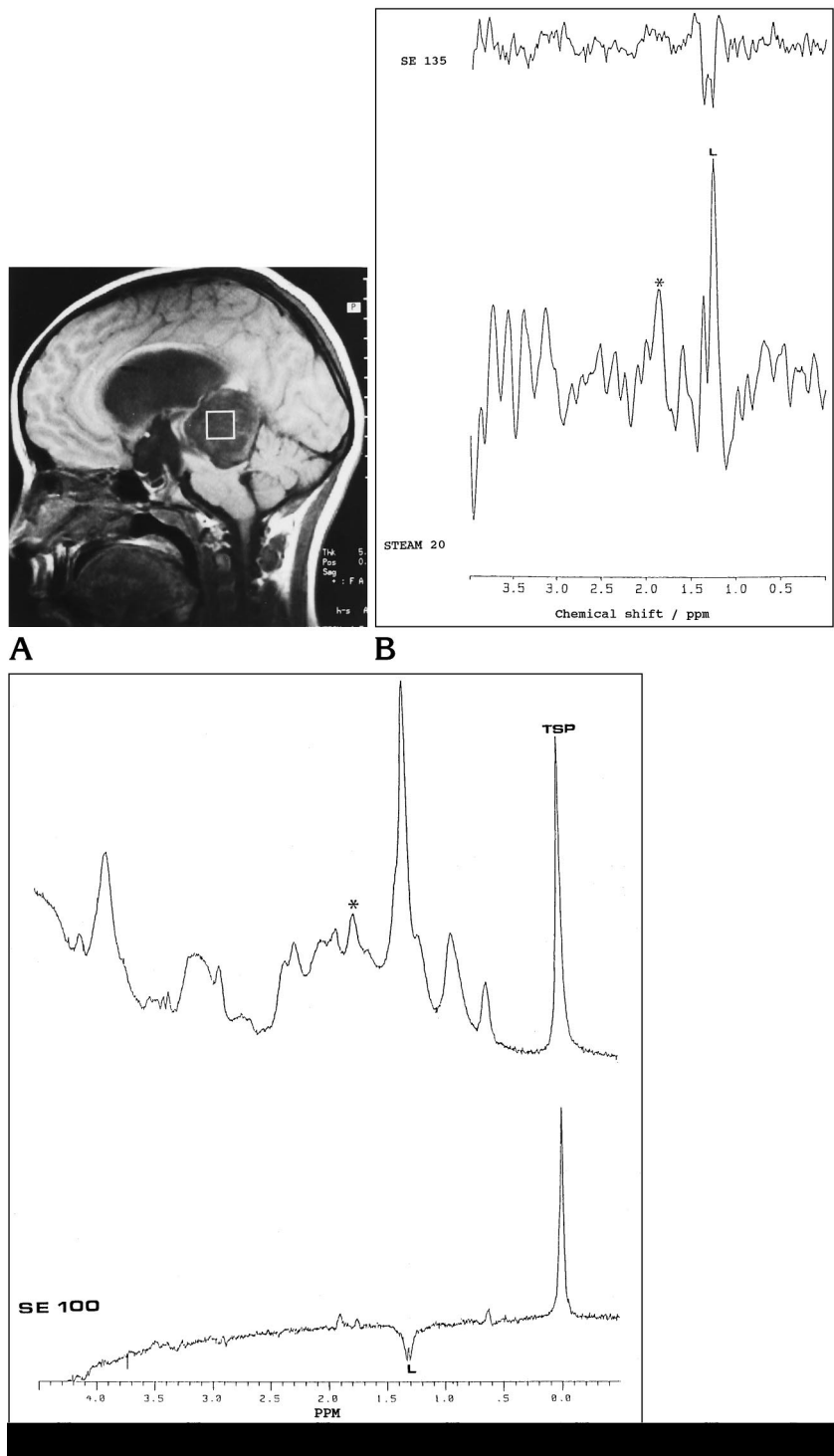
Fig 4. Meningiothelial meningioma. A, T2-weighted axial image (2200/80/1) shows well-defined, predominantly hypointense mass with areas of hyperintensity in the left parietooccipital region.

B, Spectrum at STEAM 20 shows resonances at 1.3 ppm and 1.5 ppm and a large resonance at 3.22 ppm. At spin-echo (SE) 135, the resonances of 1.3 ppm and 1.5 ppm show phase reversal compared with the Cho peak. L indicates lactate; al, alanine.

Resonance in Medicine, Berlin, August 14, 1992.). Ex vivo studies have confirmed the presence of mobile lipids in necrotic and viable tissues of high-grade gliomas and have suggested correlation between the amount of lipid and the degree of necrosis seen on histology (22, 27). Lazeyras et al ("New Perspectives in Tumor Grading," 1992) concluded that lipid signals may be useful to discriminate high- and low-grade gliomas. Necrosis distinguishes high-grade from low-grade gliomas in majority of the histologic classification system and correlate inversely with survival time (28). Necrotic areas smaller than $3 \times 3 \times 6 \text{ mm}^3$ are known to contribute significant lipid signals on proton MR spectroscopy, which are usually below the MR resolution capability (27). We have observed lipid resonances in MR-visible and -invisible necrosis in a majority of high-grade gliomas and not even in a single case of low-grade glioma. In two of our patients, although the NAA/Cho ratio was in the range of low-grade glioma (Fig 2),

the presence of lipids in these cases suggested necrosis and higher grade of malignancy. Based on the above observations, we feel that high-grade gliomas can be differentiated from low-grade gliomas on the basis of NAA/Cho and Cho/Cr ratios, along with the presence of lipids or lactate and lipids.

Metastases are known to show variable Cho and Cr, and low or absent NAA, lipids, lactate, or lipids and lactate (7-9, 11, 23). The presence of NAA in metastases, on in vitro and in vivo studies, is attributed to the presence of normal brain parenchyma in infiltrating lesions or the partial volume effects with adjacent brain tissue (8, 9, 25). The presence of a small broad resonance at 2.02 ppm, in five cases, along with resonances at 1.3 ppm and 0.9 ppm is probably attributable to the β methylene protons of lipids, because these resonances disappeared on sequences with higher echo times. Recently, similar observations have been made by ex vivo studies on different tumors (22, 27). We have



observed broad signal comprising both lipids and lactate in all seven cases and Cho in four of seven cases. Presence of lipids may be related to tissue necrosis as seen in high-grade malignancy (22). The spectral pattern in metastases was similar to that in high-grade gliomas and

lymphomas. Similar observations also have been made by Ott et al (11).

The presence of alanine is considered specific for meningiomas (4, 6). However, Kugel (9) has found alanine in only 5 of 8 cases, and Ott (11) has shown its presence in only 4 of 11